Please cite this article as:
Heidari M, Kotsovinos P, Rein G. Flame extension and the near field under the ceiling for travelling fires inside large compartments. Fire and Materials. SPECIAL ISSUE. 2019 :1–14. https://doi.org/10.1002/fam.2773

Title: **Flame Extension and the Near field under the Ceiling for Travelling Fires inside Large Compartments**

Mohammad Heidari[1, 3], Panagiotis Kotsovinos[2], and Guillermo Rein[3] ✉

[1]*Fire Testing Centre, CERIB, France*

[2]*Arup, UK*

[3]*Department of Mechanical Engineering, Imperial College London, London SW7 2AZ, UK*

ABSTRACT

Structures need to be designed to maintain their stability in the event of a fire. The travelling fire methodology (TFM) defines the thermal boundary condition for structural design of large compartments of fires that do not flashover, considering near field and far field regions. TFM assumes a near field temperature of 1200 °C, where the flame is impinging on the ceiling without any extension and gives the temperature of the hot gasses in the far field from Alpert's correlations. This paper revisits the near field assumptions of the TFM and for the first time includes horizontal flame extension under the ceiling, which affects the heating exposure of the structural members thus their load-bearing capacity. It also formulates the thermal boundary condition in terms of heat flux rather than in terms of temperature as it is used in TFM, which allows for a more formal treatment of heat transfer. The Hasemi, Wakamatsu and Lattimer models of heat flux from flame are investigated for the near field. The methodology is applied to an open-plan generic office compartment of 960 m² floor area and 3.60 m high with concrete, and with protected and unprotected steel structural members. The near field length with flame extension (fTFM) is found to be between 1.5 and 6.5 times longer than without flame extension. The duration of the exposure to peak heat flux, depends on the flame length, which is 53 min for fTFM compared to 17 min for TFM, in the case of a slow 5% floor area fire. The peak heat flux ranges from 112 to 236 kW/m² for the majority of fire sizes using the Wakamatsu model, and from 80 to 120 kW/m² for the Hasemi and Lattimer models, compared to 215 to 228 kW/m² for TFM. The results show that for all cases, TFM results in higher structural temperatures compared to different fTFM models (600°C for concrete rebar and 800°C for protected steel beam), except for the Wakamatsu model that for small fires sizes leads to approximately 20% higher temperatures than TFM. These findings mitigate the uncertainty around the TFM near field model and confirm that it is conservative for calculation of the thermal load on structures. This study contributes to the creation of design tools for better structural fire engineering.

Keywords: fire dynamics, fire safety, flame, heat flux, heat transfer, thermal analysis, structures, travelling fire

Nomenclature	
d	thickness of insulation [m]
D	diameter of the fire [m]
F	surface area of member [m²]
H	ceiling height above fire source [m]
h	convective coefficient [W/m²]
K	concrete conductivity [Wm/K]
L	length of the compartment [m]

Please cite this article as:
Heidari M, Kotsovinos P , Rein G. Flame extension and the near field under the ceiling for travelling fires inside large compartments. Fire and Materials. SPECIAL ISSUE. 2019 :1–14. https://doi.org/10.1002/fam.2773

L_H	horizontal flame length along the ceiling [m]
L_f	length of the fire [m]
L_t*	dimensionless length of the fire
Q	heat release rate [W]
Q^*	dimensionless heat release related to height H of the compartment
Q^*_D	dimensionless heat release related to the diameter D of the fire
Q^*_L	dimensionless heat release related to fire length L of fire at time t
Q″	heat release rate per unit area [W/m^2]
q_f	fuel load density [J/m^2]
q''_c	received heat flux to the ceiling [kW/m²]
q''_{net}	net heat flux [kW/m²]
q''_{rad}	net heat flux to unit surface area due to radiation [kW/m²]
q''_{con}	net heat flux to unit surface area due to convection [kW/m²]
q''_g	gauge heat flux [kW/m²]
r	horizontal distance between the centerline axis of the fire and a point along the ceiling
s	flame spread rate [m/s]
s_{min}	maximum fire spread rate [m/s]
s_{max}	minimum fire spread rate [m/s]
T_f	fire temperature [°C]
T_s	surface temperature [°C]
T_g	gas temperature [°C]
T_∞	ambient temperature [°C]
T_{ff}	far field temperature [°C]
T_{nf}	near field fire temperature [°C]
T_i^t	concrete temperature at instantaneous time t and location i [°C]
t	time [s]
t_b	local burning time [s]
t_t	total fire duration [s]
V	volume of steel per length [m^3]
W	width of the compartment [m]
x	location of interest in the compartment [m]
x·	location of the leading edge of the fire relative to the end of the compartment where fire started [m]
y	normalized distance along ceiling
z’	virtual origin of fire [m]
Φ	view factor
ε_f	emissivity of the flame of the fire
ε_s	surface emissivity
ΔT_m	change in steel member temperature
Δt	time step [s]
Δx	element length [m]
c	specific heat [J/kgK] (i: insulation, s: steel; c: concrete)
ρ	density [kg/m^3] (i: insulation, s: steel; c: concrete)
σ	Stephan Boltzmann constant (=5.67·10^{-8} [W/m^{2}K^4])

Please cite this article as:
Heidari M, Kotsovinos P , Rein G. Flame extension and the near field under the ceiling for travelling fires inside large compartments. Fire and Materials. SPECIAL ISSUE. 2019 :1–14. https://doi.org/10.1002/fam.2773

1 INTRODUCTION

In large open plan spaces, fires have been observed to travel across the compartment floor leading to fire durations of several hours and a non-uniform thermal environment inside the compartment.[1] Such fires have been referred to as Travelling Fires. The concept of the Travelling Fires Methodology (TFM) has progressed in the last decade particularly to characterize the possible thermal environment for structural design purposes.[1–3] One of the recently developed methodologies is iTFM.[3] The methodology considers a family of possible travelling fires, where each fire has a different burning area and spread rate. Thermal conditions from the family of fires allow selecting the most challenging scenario for structural design. It is important to note that travelling fire methodology is not predictive and is intended to be used as a complementary tool by designers when undertaking structural fire engineering analyses for robustness in addition to traditional design fires.[4–7] TFM considers the near field and far field regions of a fire.[2,3] As the fire travels throughout the compartment, the structural elements at the ceiling level experience the thermal exposure from the far field and near field regions.[2,3] The near field temperature, where the flame is impinging on the ceiling, ranges from 800°C – 1200 °C (1200 °C generally adopted for conservativeness). The hot gas temperature in the far field can be calculated by Alpert's correlations,[8] which were developed from fire tests with an unconfined ceiling.[9] Recent experiments such as x-ONE and x-TWO,[10] and the Malveira Fire Test[11] investigate large compartment fire dynamics to improve the current understanding. TFM can be further improved as more experiments become available.

The assumptions in the Travelling Fire Methodology produce a simple and reasonable representation of travelling fire scenarios that can be used conservatively for structural design. The methodology does not intend to represent all process related to fire dynamics in large compartments, which further research is still required. This paper revisits the near field assumption of TFM and includes the flame extension under the ceiling. It thus considers the full extension of the near field region, which affects the heating exposure to the structural members. This new concept is labelled in this paper as traveling fire with flame extension (fTFM).

TFM has traditionally been expressed in terms of gas temperatures; rather than heat fluxes.[2,3] This is to provide a simple thermal boundary condition that can be readily used by structural engineers, following the standard of the ISO834[12] and EN 1991-1-2[13] parametric design fires that are traditionally adopted in design. These traditional design fires assume uniform temperature and a uniform burning conditions,[13] which are not valid for large compartments.[1] In addition, the standard fire can only be used for comparative design purposes. The use of temperature is generally appropriate for heat transfer within the gas phase.[14,15] However, in order to consider the flame extension under the ceiling, the boundary conditions are best to be expressed in terms of incoming heat fluxes. Available methodologies describing flame extension under the ceiling utilize heat flux in their expressions. Heat flux is an appropriate boundary condition that can be used to determine the structural element temperature and thus structural behavior. This is discussed by Torero et al.,[15] since the thermal boundary conditions at the exposed surface of a structural element are based on conservation of energy.

Please cite this article as:
Heidari M, Kotsovinos P , Rein G. Flame extension and the near field under the ceiling for travelling fires inside large compartments. Fire and Materials. SPECIAL ISSUE. 2019 :1–14. https://doi.org/10.1002/fam.2773

In this paper, a methodology to calculate the horizontal flame length under the ceiling is investigated, thus allowing to determine the heat flux along the length of flame under the ceiling; in turn improving the near field assumption of TFM to obtain a better boundary condition for a surface exposed to a travelling fire. A comparison for a generic open plan office compartment is presented. The thermal response of a concrete slab, and protected and unprotected steel beams subjected to travelling fire with flame extension (fTFM) is studied based on three different heat flux calculation methodologies, along with iTFM and the EN 1991-1-2 parametric fire curve.

2 FLAME EXTENSION IN COMPARTMENT FIRES

When the flame height exceeds the ceiling height, a part of the flame deflects horizontally and becomes a part of a shallow layer under the ceiling the carries heat and smoke to the area far from the fire location (i.e. ceiling jet). The flame length below the ceiling controls the heat transfer to the ceiling from the flame. Studies on flame extension under a non-combustible ceiling[14,16] suggest that the ratio of the horizontal part of the flame to the cut-off height due to the presence of a ceiling, could range from 0.88 to 12, depending on the configuration involved. A considerable flame extension can occur when the fire is large in comparison to the ceiling height as discussed by Drysdale. [14]

Hasemi et al.[17] studied the behavior of flame under an unconfined ceiling during a set of experiments and found that the flame length under the ceiling data could be correlated with non-dimensional heat release rate, given by:

$$L_H = 2.9H \cdot (Q^*)^{0.33} - H \quad (1)$$

$$Q^* = Q / (1.11 \cdot 10^{-6} \cdot H^{5/2}) \quad (2)$$

where L_H [m] is the horizontal flame length along the ceiling away from the symmetrical flame axis, H [m] is the ceiling height above fire source, Q is the heat release rate [W], and Q^* is the non-dimensional heat release rate. These equations, which are adopted in EN 1991-1-2 (Annex C) investigated in this paper. Other methods are also available to calculate the horizontal part of flame under the ceiling, depending on the configuration.[18]

Hasemi et al.[17] also carried out experiments to measure the incident heat flux from a localized fire to an unconfined flat ceiling located above the different size of propane burners (0.3m, 0.5m, and 1m in diameter) (Figure 1 (a)). Their study considers heat release rates and ceiling heights and measured the incident heat flux to the ceiling from fire and fire plume impinging on the ceiling. They measured heat flux at different locations r from the flame centreline axis, using heat flux gauges. The peak heat flux of 100 kW/m² was measured at the stagnation point (the symmetrical flame axis) as illustrated in Figure 1 (b).

Please cite this article as:
Heidari M, Kotsovinos P , Rein G. Flame extension and the near field under the ceiling for travelling fires inside large compartments. Fire and Materials. SPECIAL ISSUE. 2019 :1–14. https://doi.org/10.1002/fam.2773

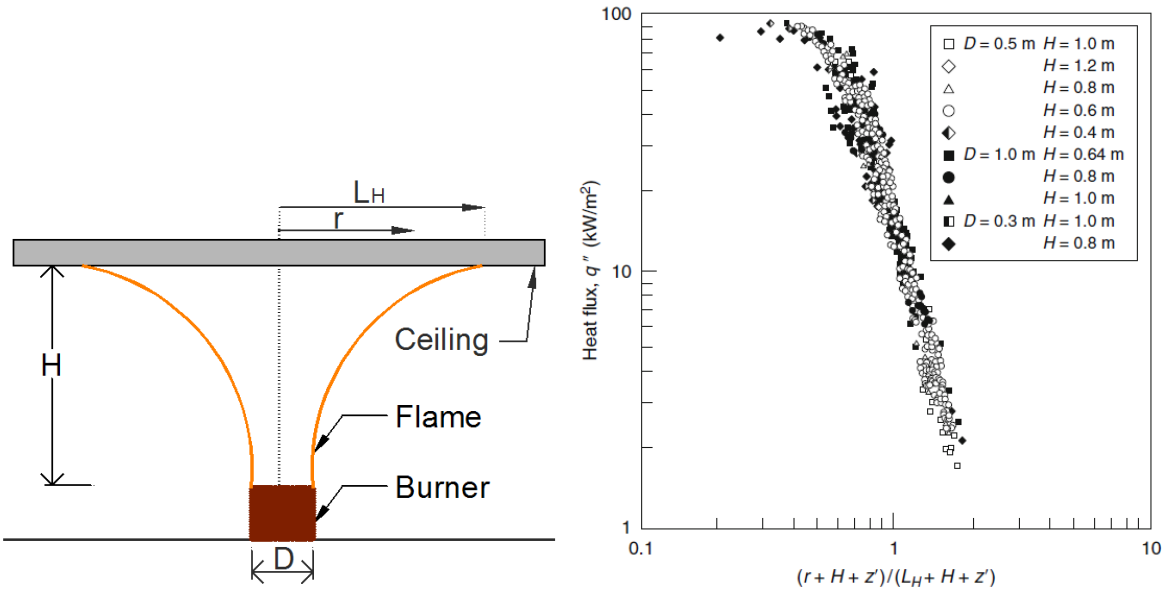

(a) **(b)**

Figure 1 (a) Sketch of a flame impinging on the ceiling and extending horizontally. (b) Measured heat fluxes under an unconfined ceiling from an impinging buoyant diffusion flame reported by Hasemi et al.[17] L_H is the flame extension under the ceiling, given by Eq. 1. y is the normalized distance of the studied point from the virtual fire source (see Equation 4)

Further experiments[19] with heat release rates of up to 61 MW and fire surface area of 150 m² using wood and polystyrene, showed a good prediction of the Hasemi model in the area above the fire zone and presented the following expressions to determine the received heat flux to the ceiling from localized fires flame when the flame is impinging on the ceiling:

$$q''_c = \begin{cases} 100 & \text{for } y \le 0.3 \\ 136.3 - 121y & \text{for } 0.3 < y \le 1 \\ 15y^{-3.7} & \text{for } y > 1 \end{cases} \quad (3)$$

$$y = (r+H+z') / (L_H+H+ z') \quad (4)$$

$$z' = 2.4D \cdot (Q^*_D{}^{2/5} - Q^*_D{}^{2/3}) \quad \text{for } Q^*_D < 1 \quad (5)$$

$$z' = 2.4D \cdot (1 - Q^*_D{}^{2/5}) \quad \text{for } Q^*_D \ge 1 \quad (6)$$

$$Q^*_D = Q / (1.11 \cdot 10^{-6} \cdot D^{5/2}) \quad (7)$$

where q''_c [kW/m²] is the incident heat flux at the ceiling, r [m] is the horizontal distance [m] between the centerline axis of the fire and a point along the ceiling where the thermal flux is calculated, y is the normalized distance of the studied point along the ceiling from the virtual fire source, H [m] is the ceiling height above fire source, z' [m] is the virtual origin of fire, Q^*_D is the non-dimensional heat release rate, and D [m] is the diameter of the fire (see Figure 1 (a)). These expressions were adopted by EN 1991-1-2[13] to calculate the horizontal flame

Please cite this article as:
Heidari M, Kotsovinos P , Rein G. Flame extension and the near field under the ceiling for travelling fires inside large compartments. Fire and Materials. SPECIAL ISSUE. 2019 :1–14. https://doi.org/10.1002/fam.2773

extension under the ceiling, and thus the heat flux received by the fire exposed unit surface area at the level of the ceiling.

Wakamatsu et al.[18] also studied the same problem and presents a correlation for the incident heat flux to the ceiling as a function of y, the normalize distance of the studied point from the virtual fire source, given by:

$$q''_c = 518.8e^{-3.7y} \quad (8)$$

The heat flux measurements in the Myllymaki[20] experiments from fires impinging on I-beam mounted to a ceiling, using heptane pool fires and different ceiling heights, show a good agreement between the Wakamatsu equation and the tests data. Lattimer[18] reviewed a number of studies on thermal conditions produced by fires impinging on the ceiling. He discussed the methods to determine the heat flux boundary condition for structural members at the level of the ceiling. Based on the data from Hasemi[17] and Myllymaki[20] experiments, Lattimer[18] presents the following equations to calculate the incident heat flux to an unconfined ceiling.

$$q''_c = 120 \quad \text{for } y \leq 0.5 \quad (9)$$

$$q''_c = 682e^{-3.4y} \quad \text{for } y > 0.5 \quad (10)$$

The model by Lattimer[18] sets the peak heat flux to 120 kW/m² at y less than or equal 0.5, unlike the Wakamatsu et al.[18] model that does not have a peak heat flux as plotted in Figure 2. The curve from Wakamatsu Eq. and the data from Hasemi et al.[17] are illustrated in Figure 2 for comparison. It can be seen that the Wakamatsu Eq. and the test data are almost in the same range when y is greater than 0.45, but the Wakamatsu Eq. overestimate the heat flux for smaller values of y.

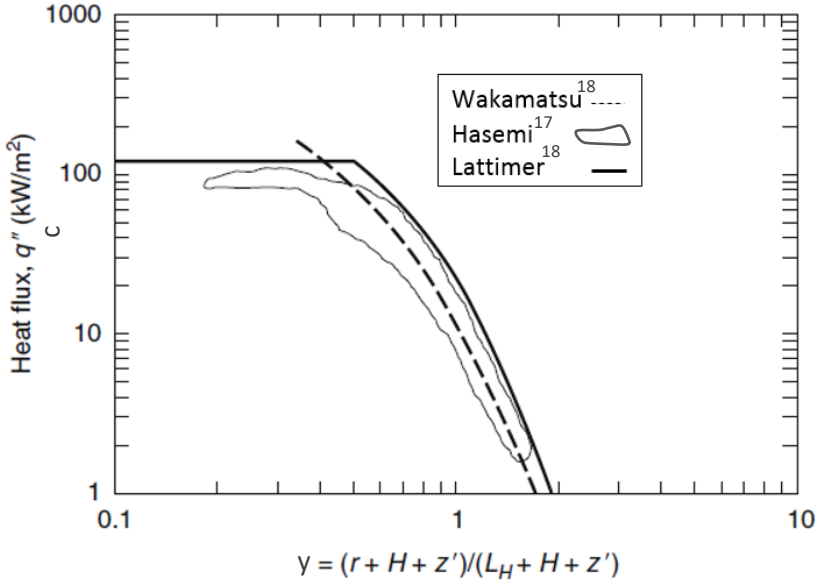

Figure 2 From[18], a comparison of the data from Hasemi et al.[17] (outlined area), the dashed line represents the Wakamatsu and the continuous line represents the bounding fit to the data from Hasemi and Wakamatsu.

Please cite this article as:
Heidari M, Kotsovinos P , Rein G. Flame extension and the near field under the ceiling for travelling fires inside large compartments. Fire and Materials. SPECIAL ISSUE. 2019 :1–14. https://doi.org/10.1002/fam.2773

For comparative purposes and given that the flame extension has not been studied for travelling fires, all three models available in the literature, Hasemi, Wakamatsu, and Lattimer, will be investigated in this study. All models will be combined individually with iTFM to consider flame extension (fTFM) and determine the heat flux boundary condition under the ceiling to the structural elements. It should be noted that the calculated heat flux here does not apply to columns.

3 TRAVELLING FIRES WITH FLAME EXTENSION

3.1 Background to TFM

TFM[2,3] produces a temporally and spatially non-uniform temperature distribution. The methodology can consider a range of possible flame lengths, L_f [m], which is equivalent as fire diameter (D) in 1D compartment, by assuming different fire spread rates, s [m/s]. These spread rates control the time required for the leading edge of the fire to travel while the trailing edge of the fire is governed by the time required for the fuel to burn-out (t_b). The flame length, L_f, is therefore defined as:

$$L_{f\,min/max} = s_{min/max} \cdot t_b \quad (11)$$

$$t_b = q_f / Q'' \quad (12)$$

Fire spread rates between 0.1 and 19 mm/s have been determined from various experiments conducted to date on wood crib fires. The range of possible fire sizes is from $L_{f\,min}/L$ to $L_{f\,min}/L$, where L [m] is the length of the compartment. t_b [s] is the local burning time, which is a function of the fuel load density, q_f [J/m²], and the heat release rate per unit area Q'' [W/m²].

Total fire duration t_t [s], and location of the leading edge of the fire relative to the end of the compartment where the fire started $x^{\cdot}$ [m], can be calculated as follow:

$$t_t = t_b \cdot (L/L_f+1) \quad (13)$$

$$x^{\cdot} = s \cdot t \quad (14)$$

TFM assumes that the fire travels throughout the compartment and structural elements at the ceiling level see the impact of the far field and near field temperature. The far field temperature, where the hot gas temperature is estimated, is calculated by Alpert's correlations, [9] which were developed based on set fire tests with an unconfined ceiling, with heat release rate ranging from 600 kW to 98 MW (Figure 3). TFM uses Alpert's correlation for the reason of simplicity since the difference between Alpert's correlation and other available methods for far field temperature are negligible and considering the additional complexity, computational time required and uncertainty in the parameters associated with other methods.[3] The far field temperature T_{ff} [°C], is obtained by the following expressions:

$$T_{ff} = T_\infty + 5.38/H \cdot [(L \cdot L_t^* \cdot W \cdot Q'' \cdot 10^{-3})/ (|x + 0.5L \cdot L_t^* - x^{\cdot}_t|)]^{2/3} \quad (15)$$

$$\text{For } x^{\cdot} \le L \rightarrow x^{\cdot}_t = s \cdot t;\ L_t^* = \min [L_f/L, s \cdot t/L] \quad (16)$$

Please cite this article as:
Heidari M, Kotsovinos P , Rein G. Flame extension and the near field under the ceiling for travelling fires inside large compartments. Fire and Materials. SPECIAL ISSUE. 2019 :1–14. https://doi.org/10.1002/fam.2773

For $x^{\cdot} > L \rightarrow x^{\cdot}_t = L$; $L_t^* = 1 + (L_f - s \cdot t)/L$ (17)

where T_∞ [°C] is the ambient temperature, W [m] is the width of the compartment, x [m] is the location of interest in the compartment from the ignition point, $x^{\cdot}_t$ [m] is the location of the leading edge of the fire at time step t [s], and L_t^* is the varying dimensionless fire size which depends on the location of the leading edge of the fire.

TFM assumes the near field temperature to be T_{nf}=1200°C. The phenomenon of flame flapping can be incorporated, which considers a non-vertical flame resulting from ventilation and turbulence. This flapping phenomenon includes the cooler smoke with the fluctuating flame, calculated by Alpert's correlation, into near field temperature and decreases the near field temperatures for small fire sizes. A flapping angle of Θ= ±6.5° is typically assumed in iTFM. [3] The equation used to calculate the reduced near field temperature due to flapping is a combination of near field temperature and Alpert's correlation.[3] The flapping effect is incorporated in travelling fire with flame extension.

3.2 TFM with Flame Extension (fTFM)

TFM bounds the near field (i.e. the flame region) to the flapping length under the ceiling and does not consider the flame extension beyond this region. In reality, the fire could extend a few meters under the ceiling. Therefore, the structural elements would experience more intense heating under the direct impact of the flame instead of the hot gases. This paper includes the flame extension into TFM and extends the formulation of the near field region of the TFM, which allows for a better resolution of the near field.

The flame extension equation (Eq. 1) is a function of the non-dimensional heat release rate, and subsequently is a function of the heat release rate. Considering this, the non-dimensional heat release rate can be calculated as follows, using the heat release rate from TFM:

$$Q^* = (L \cdot L_t^* \cdot W \cdot Q'')/(1.11 \cdot 10^{-6} \cdot H^{5/2}) \quad (18)$$

where Q'' [W/m²] is the heat release rate per unit area. Eqs. (16) and (17) are used to define varying fire size and location of the leading edge based on whether fire is still increasing in size or at its maximum size (Eq. (16)), or has reached the far end of the compartment and is decaying (Eq. (17)). Combination of flame extension equation under the ceiling (Eq. 1) and Eq. 18 results in the flame extension under the ceiling for travelling fire at time t during the fire:

$$L_H(t) = 2.9H \cdot (Q^*)^{0.33} - H \quad (19)$$

It should be noted that TFM is used to find the gas temperature distribution at all locations in the compartment when the fire is spreading in one direction and covering the complete width of the compartment. Therefore, Eq. 19 defines the flame extension under the ceiling in the direction that fire is moving. This allows one to calculate the heat flux from the extended flame under the ceiling to the structural elements, using available methods to calculate the heat flux. The methodologies in section 2; Hasemi, Wakamatsu, and Lattimer, are used to define the distribution of received heat flux to the ceiling from the fire, over the near field region. Figure 3 shows an illustrative example of the final heat flux-temperature curve using

Please cite this article as:
Heidari M, Kotsovinos P , Rein G. Flame extension and the near field under the ceiling for travelling fires inside large compartments. Fire and Materials. SPECIAL ISSUE. 2019 :1–14. https://doi.org/10.1002/fam.2773

iTFM with flame extension under the ceiling, which is explained further below. Figure 3 illustrates the near field with flame extension, which has a length twice the flame extension length under the ceiling. The far field temperature beyond the flame region under the ceiling is calculated using Alpert's correlation, as in TFM. The far field temperature is then converted to the received heat flux to a cold surface to be consistent with the definition of heat flux of Hasemi, Wakamatsu and Lattimer models. This heat flux conversion is a novel contribution of this work and is discussed in detail in section 3.3.

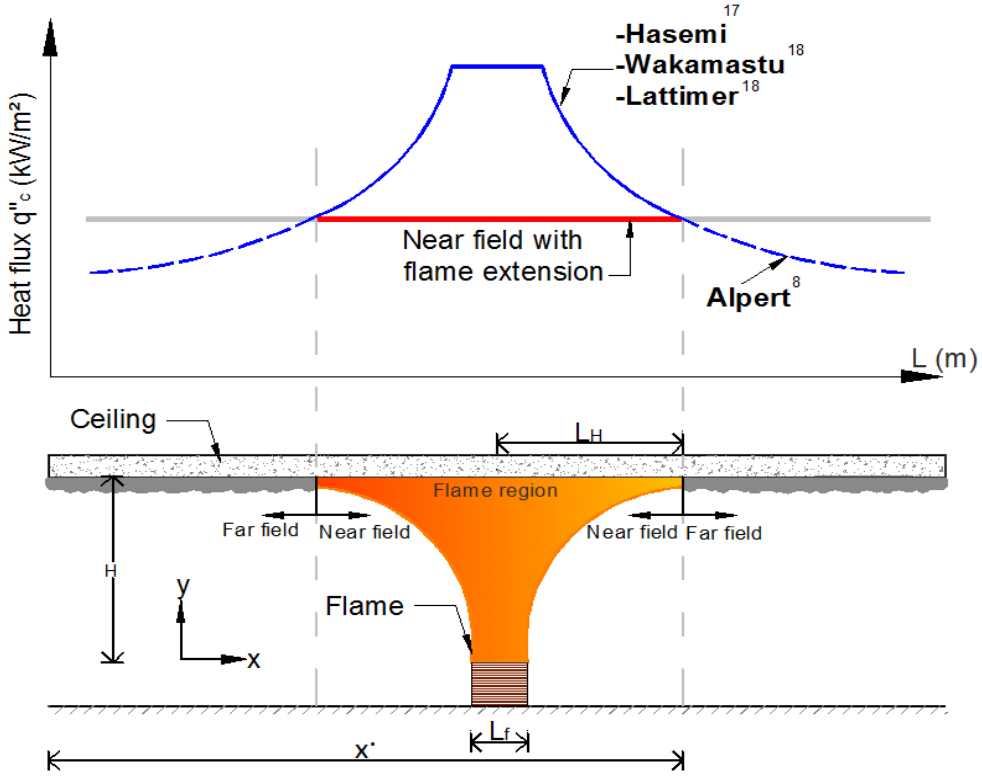

Figure 3 Schematic of TFM with flame extension under the ceiling. For the near field region with flame extension, the heat flux is calculated from Hasemi, Wakamatsu and Lattimer models. For the far field, the heat flux to a cold surface were calculated from TFM far field temperature. L is the length of compartment.

The received heat flux to the ceiling in the near field region, as illustrated in Figure 3, at a location x and time t of interest could be then expressed as below for the three different models.

1. Hasemi :

$$q''_c(x,t) = \begin{cases} 100 & \text{for } y_t \le 0.3 \\ 136.3 - 121 y_t & \text{for } 0.3 < y_t \le 1 \\ 15 y_t^{-3.7} & \text{for } y_t > 1 \end{cases} \quad (20)$$

2. Wakamatsu :

$$q''_c(x,t) = 518.8 e^{-3.7 y_t} \quad (21)$$

3. Lattimer :

$$q''_c(x,t) = 120 \quad \text{for } y_t \le 0.5 \quad [W/m^2] \tag{22}$$

$$q''_c(x,t) = 682e^{-3.4y_t} \quad \text{for } y_t > 0.5 \quad [W/m^2]$$

The horizontal distance between the centerline vertical axis of the travelling fire and a point along the ceiling at each time step, r_t [m], and the fire size, L_f [m], in accordance with iTFM are given by:

$$r_t = |x + 0.5L \cdot L_t^* - x'_t| \tag{23}$$

$$L_f = 0.5L \cdot L_t^* \tag{24}$$

A point of studied with distance x from the ignition point is considered in the flame region (near field) when $r_t < L_H(t)$, therefore equations 20 to 22 could be applied to calculate the received heat flux to the point of studied.

The normalized distance of the point of interest from the virtual fire source, y_t, the virtual source location, z'_t (m), and Q^*_L is the non-dimensional heat release rate at time t during the fire can be calculated as follow:

$$y_t = (r_t+H+Z) / (L_H(t)+H+Z) \tag{25}$$

$$z'_t = 2.4\, L_f \cdot (Q^*_L{}^{2/5} - Q^*_L{}^{2/3}) \quad \text{for } Q^*_L<1 \tag{26}$$

$$z'_t = 2.4\, L_f \cdot (1 - Q^*_L{}^{2/5}) \quad \text{for } Q^*_L \ge 1 \tag{27}$$

$$Q^*_L = (L \cdot L_t^* \cdot W \cdot Q'') / (1.11 \cdot 10^{-6} \cdot L_f^{5/2}) \tag{28}$$

It is important to It should be noted that the nomenclature of “iTFM+Hasemi (iTFM+Ha)”, “iTFM+Wakamatsu (iTFM+Wa)” and “iTFM+Lattimer (iTFM+La)” is adopted for the different models with flame extensions included and determined in accordance with equations 20, 21, and 22 respectively.

For clarity, Figure 4 (a) shows an illustrative example of the received heat flux to a structural member at the ceiling level for an arbitrary location in a compartment, using the methodology presented in this paper. The heat flux calculated from iTFM is also plotted. The combination of near field, calculated by Hasemi model, and far field from iTFM provide the total heat flux boundary condition (Figure 4 (b)).

It should be noted that the maximum heat flux between those calculated from Hasemi model and iTFM were selected for the near field with extension flame, assuming the peak heat flux is always below 100 kW/m² (the peak heat flux prediction of Hasemi model). This is because the heat flux from a flame cannot be lower than the heat flux from the hot gas.

In the same way, the heat flux-time curve could be generated using Wakamatsu (Eq. 21) and Lattimer (Eq. 22) models, assuming that the peak heat flux with Lattimer model is 120 kW/m² while there is no peak heat flux limit for the Wakamatsu model.

Please cite this article as:
Heidari M, Kotsovinos P , Rein G. Flame extension and the near field under the ceiling for travelling fires inside large compartments. Fire and Materials. SPECIAL ISSUE. 2019 :1–14. https://doi.org/10.1002/fam.2773

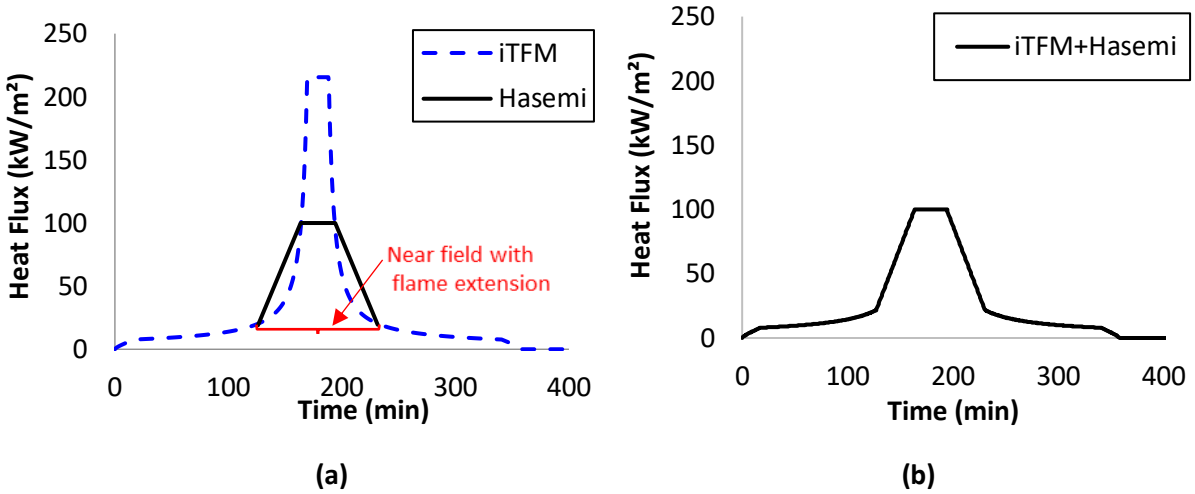

Figure 4 illustrative example of, (a) the heat flux at the ceiling level for an arbitrary location in a compartment using iTFM compared to the methodology with flame extension, (b) the final heat flux boundary condition in accordance with fTFM, combining the far field from iTFM and the near field from Hasemi.

3.3 Heat Flux Boundary Condition

As discussed in section 1 and shown by Torero et al.,[15] heat flux is a thermally accurate way to define the boundary condition at the exposed surface of the structural element as temperature may not always be appropriate.[15] In this section, the heat flux concepts are reviewed to extract the relevant parameters needed to convert the gas temperature from TFM to heat flux. The standard definitions and principles of the heat transfer phenomena are not described here and can be found in Incropera et al.[21]

The net heat flux boundary condition consists of heat transfer by convection (q''_{con}) and radiation (q''_{rad}) from fire to the solid surface:

$$q''_{net} = q''_{rad} + q''_{con} = \varepsilon_s \cdot \varepsilon_f \cdot \sigma \cdot \Phi \cdot [(T_g + 273)^4 - (T_s + 273)^4] + h\,(T_g - T_s) \quad (29)$$

where ε_s and ε_f are the surface and fire emissivities, σ is the Stephan Boltzmann constant (= $5.67 \cdot 10^{-8}$ W/m^{2}K^4), Φ is the view factor, T_s and T_g are the surface and the gas temperature respectively, and h [W/m²] is the convective coefficient. Hasemi et al.[17] used a water-cooled heat flux gauge during the experiments to measure the maximum received heat flux. These gauges are cooled so that their surface temperature (T_s) remains low at T_∞ in the range (20–80°C). Cooling the gauge surfaces maximizes heat transfer to the surface. Gauges are coated with high emissivity coating paint ($\varepsilon \approx 0.95$) to maximize the absorbed radiation. As such, the flux gauges measure the maximum received heat flux (q''_c). The net heat flux to a surface can be also expressed in terms of q''_c as in Eq. 30 [13,18]:

$$q''_{net} = q''_c - \varepsilon_s \cdot \varepsilon_f \cdot \sigma \cdot \Phi \cdot [(T_s + 273)^4 - (T_\infty + 273)^4] - h \cdot (T_s - T_\infty) \quad (30)$$

q''_c was measured in experiments of Hasemi[17] and Myllymaki[20]. By comparing Eq. 29 and Eq. 30, the gauge heat flux can be express as:

Please cite this article as:
Heidari M, Kotsovinos P , Rein G. Flame extension and the near field under the ceiling for travelling fires inside large compartments. Fire and Materials. SPECIAL ISSUE. 2019 :1–14. https://doi.org/10.1002/fam.2773

$$q''_c = \varepsilon_s \cdot \varepsilon_f \cdot \sigma \cdot \Phi \cdot [(T_g + 273)^4 - (T_\infty + 273)^4] + h \cdot (T_g - T_\infty) \quad (31)$$

The heat Eq. 31 is used in this paper to formulate the heat flux at the exposed surface of a structure in the far field (i.e. thermal boundary condition), assuming the worst case that the solid surface remains at ambient during heating (this relies on the fact that heating rate of the gases and solid occur at different time scales as per the parametric fires in EN1991-1-2).[15] Eq. 31 converts the far field temperature from iTFM to the heat flux consistent with the work of Hasemi[17], Wakamatsu[18] and Myllymaki[20]. Therefore, in fTFM both near and far field are expressed in a consistent manner.

4 COMPARISON FOR A GENERIC STRUCTURE

A generic steel framed composite structure with a concrete slab and steel beams (composite floor on decking) is considered in order to study the impact of TFM with flame extension (fTFM) on the thermal response of structural members. The results are compared with the thermal analysis of the same structural elements, using the TFM and the EN 1991-1-2 parametric fire (which assumes a uniform temperature inside the compartment). The structural response to thermal exposures has not been assessed in this work.

The compartment is an open-plan office building, which was a similar compartment as used before in[3], with a floor area of 960 m², 40 m long by 24 m wide and 3.6 m high (Figure 5). Staircases or any division are excluded from the definition of the compartment area and layout as described by [1,2]. The building consists of a concrete slab 180 mm deep with 38 mm concrete cover and steel beams of section UB457x191UB 133 with 7 mm high-density perlite.

The fuel load density (q_f'') and heat release rate per unit area (Q'') are taken as 511 MJ/m² and 500 KW/m² respectively.[13] The risk-based factors of EN 1991-1-2 have not been applied here and risks are assumed to be explicitly considered by the designer. The fire starts at the left side and travels along the compartment (see Figure 5).

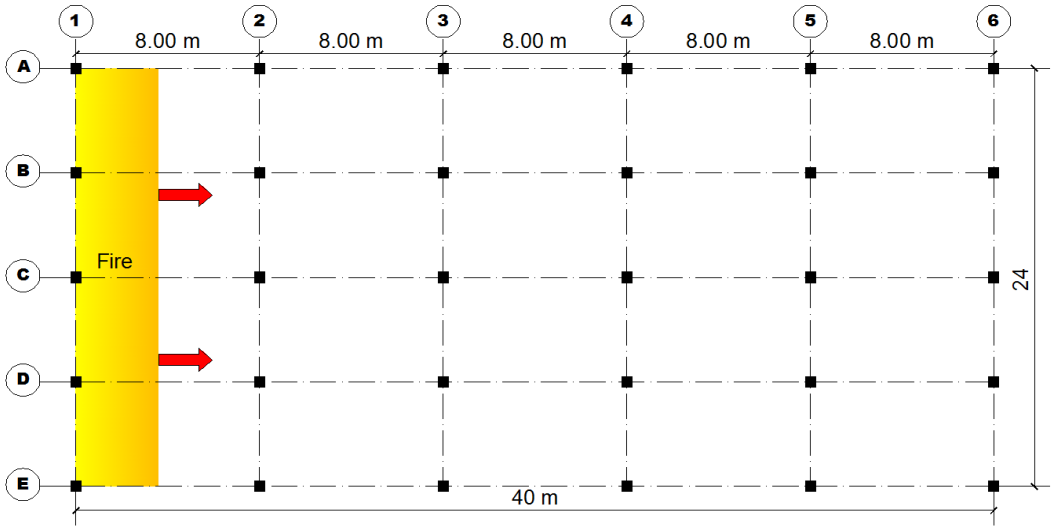

Figure 5 Plan of the structure. A-E and 1-8 are structural gridlines. Fire spans the full width of the compartment (gridlines A to E) and starts from the left-hand side of the compartment travelling at a constant spread rate to the right part of the compartment.

Please cite this article as:
Heidari M, Kotsovinos P , Rein G. Flame extension and the near field under the ceiling for travelling fires inside large compartments. Fire and Materials. SPECIAL ISSUE. 2019 :1–14. https://doi.org/10.1002/fam.2773

The thermal properties of concrete are taken as; specific heat of 1000 J/Kg K, density of 2300 Kg/m3, thermal conductivity 1.33 W/m K [22,23] with the convective heat transfer of 35 W/m² and 4 W/m² for exposed surface and backside respectively.[22,23] The thermal properties of steel are taken as,[22,24] specific heat of 600 J/Kg K, density of 7850 Kg/m^3, with a convective coefficient of 35 W/m². The thermal properties of insulation are taken as high density perlite[22] with 7 mm thickness; specific heat of 1200 J/Kg K, density of 550 Kg/m3, thermal conductivity of 0.12 W/m K. Temperature-dependent thermal properties of passive protection could result in somehow higher accuracy of the steel temperature, although for the purposes of this study and sake of simplicity, constant values were applied. Heat transfer calculations are carried out as in,[21,22] with heat flux being used as the boundary condition. In-depth concrete temperature is calculated by applying the finite-difference method for the heat conduction Eq. 32.[21] The thermal conductivity of steel is higher than concrete, therefore the steel rebar temperature is assumed to be the same as adjacent concrete. It has been shown that 1D heat transfer with constant effective properties results in conservative in-depth concrete temperature.[25] The lumped mass heat transfer method[21,22] is used for thermal analysis of the protected beam (Eq. 33) and unprotected steel beam (Eq. 34), as given by:

$$q''^{t}_{net} + K\cdot (T_1^t - T_0^t)/\Delta x = \rho_c \cdot c_c \cdot \Delta x/2 \cdot (T_1^{t+1} - T_0^t)/\Delta t \quad (32)$$

$$q''_{net} \cdot F \cdot \Delta t = \rho_s \cdot c_s \cdot V \cdot \Delta T_m \quad (33)$$

$$q''_{net} \cdot F \cdot \Delta t = \rho_s \cdot c_s \cdot V \cdot \Delta T_m + \rho_i \cdot c_i \cdot d \cdot F \cdot \Delta T_m /2 \quad (34)$$

The net heat flux, q''_{net}, are calculated from Eq. 30.

4.1 Heat Flux and Flame Extension Length

A family of fires are investigated based on typical fire spread rates observed in compartment firers (0.1 to 19.3 mm/s)[3] to generate the heat flux fields across the compartment. The corresponding fire sizes were between 0.3% and 55% of the compartment area, using Eq. 11 (i.e. fire length between 0.11 m and 22 m). The family of fire sizes account for plausible range of fuel load densities, heat release rates, fire spreads in large compartments. This allows finding the most challenging and appropriate scenarios for structural design.

The fire is assumed to be at floor level (H becomes the compartment height) and starts at the left-hand side of the compartment, spans the full width and travel over time to the right-hand side of the compartment (Figure 5). Previous studies have examined the sensitivity analysis of the input parameters and demonstrated that flame spread rates is important.[2,3] It has been shown that different fire paths and shapes do not necessarily have a significant impact on the thermomechanical response of the structure.[26]

The flame extension under the ceiling for different fire sizes is calculated at each time step, in accordance with the methodology described in this paper. Figure 6 demonstrates the relation between fire sizes and the maximum near field length with flame extension under the ceiling ($2L_H$, see Figure 3) normalized by the fire length. The normalized near field increases sharply to 6.5 for fire sizes less than 7% floor area, and then decreases to 1 for 100% fire size. Figure 7 shows how the near field length with and without flame extension vary with the size

Please cite this article as:
Heidari M, Kotsovinos P , Rein G. Flame extension and the near field under the ceiling for travelling fires inside large compartments. Fire and Materials. SPECIAL ISSUE. 2019 :1–14. https://doi.org/10.1002/fam.2773

of the fire. For example, for a 5% fire size, the near field with flame extension (fTFM) is 12.8 m while the near field calculated from TFM is 2m. The near field length with and without flame extension (fTFM and iTFM) for a 25% fire size is 26.8 m and 10 m respectively. For the 50% fire size, the near field lengths are 36 m and 20 m using the presented methodology (fTFM) and TFM without flame extension.

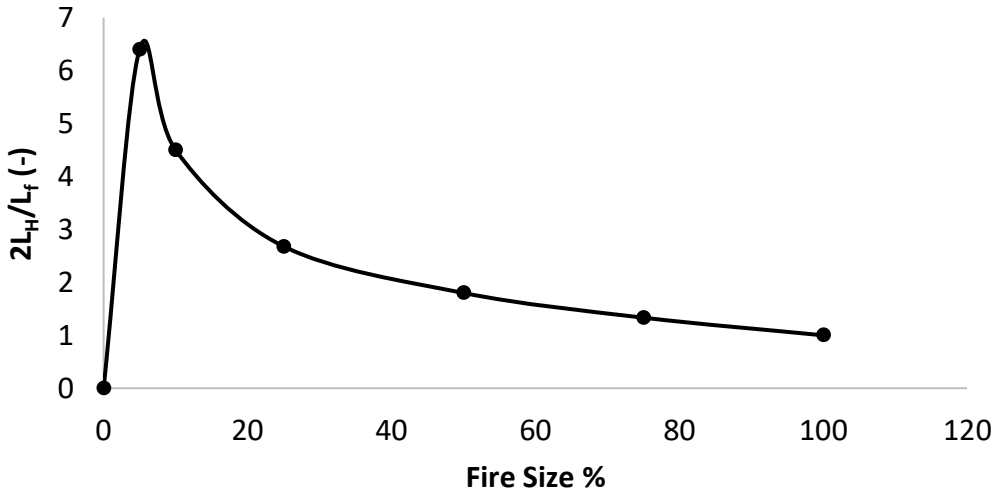

Figure 6 Ratio of flame extension length under the ceiling ($2*L_H$) over the near field length of iTFM (Lf) vs. fire size. The smaller the size of the fire, the greater the ratio.

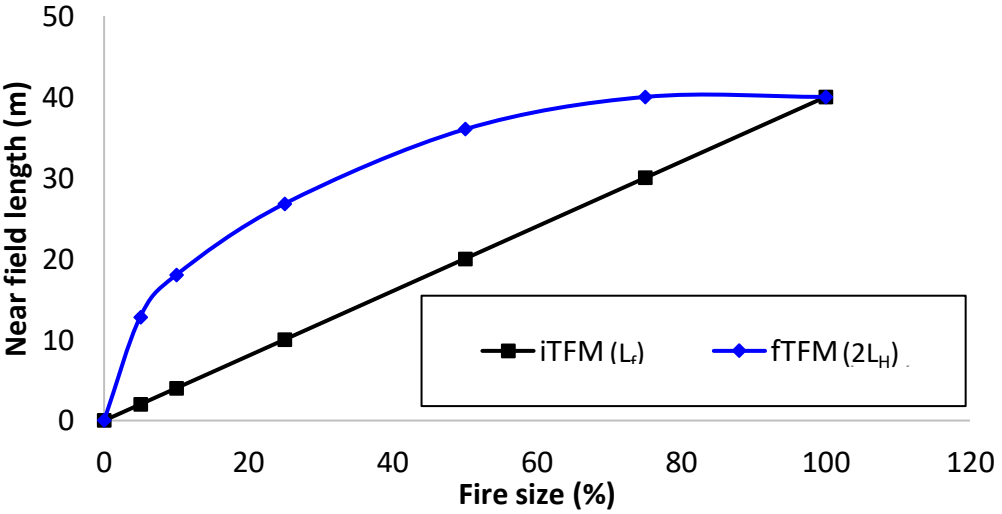

Figure 7 The near field with flame extension (fTFM) and iTFM for different fire sizes. The near field length with flame extension is considerably greater than the TFM near field.

Figure 7 illustrates that more structural elements at the ceiling could be affected by the impact of near field when the flame extension is included in TFM (by fTFM). This exposes more structural elements for longer period to the direct heat of hot flame rather than the colder hot gases of far field at any moment in time. This change in the thermal exposure could impact the resulting structural behavior, although this is not addressed in this paper. However, due to the flexibility of the travelling fire methodology with the family of travelling fires, a broader

range of fire sizes would include all potential phenomena. For this case study, a family of travelling fires is generated and investigated with sizes ranging from 5% to 55% of the floor area, in accordance with the methodology presented in this paper (fTFM). The calculated heat fluxes from the TFM are also used for comparison.

Figure 8 illustrates the received heat flux curves from a 5% of floor area travelling fire with flame extension (fTFM) and no flame extension (TFM), generated in the middle of the case study compartment. The results show how the flame extension affects the near field and far field duration.

The total burning duration is 358 min. TFM has the far field duration of 341 min and the near field duration of 17 min, with a peak heat flux of 216 kW/m². TFM with flame extension results in a total far field duration of 249 min and the near field duration of 109 min, where the Hasemi, and Lattimer result in peak heat fluxes of 100, 120 respectively. The peak heat flux from Wakamatsu is overly high and equal to 454 kW/m².

The peak heat flux using flame extension and the Wakamatsu model (iTFM+Wa) is larger than the one calculated with TFM. Flame extension with the Lattimer model (iTFM+La) and the Hasemi model (iTFM+Ha) result in a lower peak heat flux than TFM. The time that the structural element is heated by the peak heat flux varies between different models, where iTFM+La has the largest duration of 52 min, iTFM+Ha and TFM had 28 min and 17 min respectively.

It should be noted that as discussed by Lattimer[18], the Wakamatsu model does not limit the peak heat flux. Therefore, for small fire sizes, very high peak heat fluxes are experienced that may not be realistic/representative. Despite this shortcoming, they are included in this work to study the relative performance from the different models.

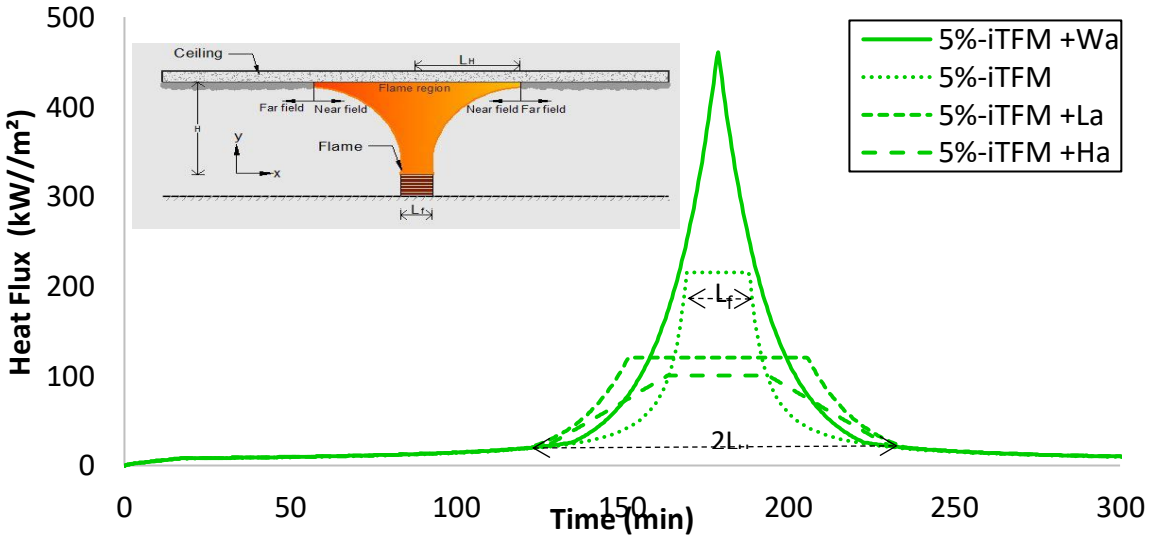

Figure 8 A comparison of TFM with and without flame extension for a 5% floor area travelling fire. Hasemi, Wakamatsu and Lattimer models were used for near field when the flame extension was included.

The heat flux-time curves and the near field durations from a family of travelling fires with and without flame extension, for a point in the middle of the compartment at the ceiling level,

Please cite this article as:
Heidari M, Kotsovinos P , Rein G. Flame extension and the near field under the ceiling for travelling fires inside large compartments. Fire and Materials. SPECIAL ISSUE. 2019 :1–14. https://doi.org/10.1002/fam.2773

are illustrated in Figure 9 to Figure 11. Eqs. 21, 22 and 23 are applied to determine the near field heat flux, in accordance with the presented methodology. The results illustrate that the lower the fire size, the longer the near field duration when the flame extension is included.

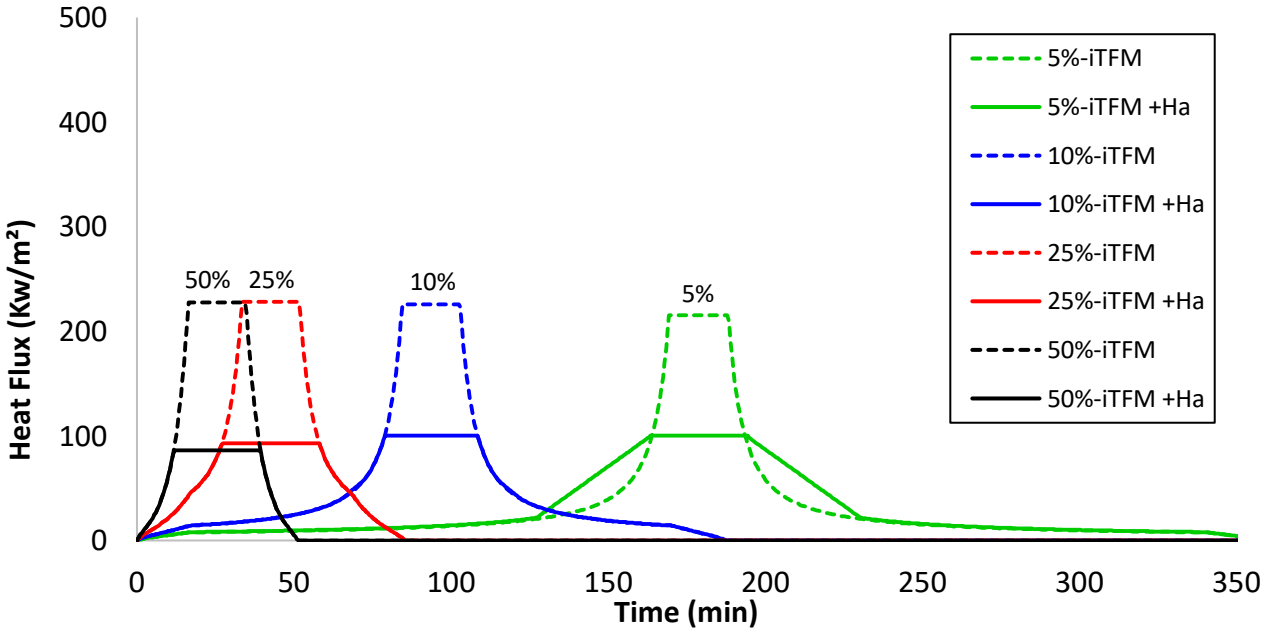

Figure 9 Heat flux received at the ceiling level in the middle of the compartment for a family of traveling fire sizes, using TFM and iTFM+Hasemi (iTFM+Ha). The peak heat flux in iTFM+ Hasemi is set to 100 kW/m², in accordance with Hasemi model. The impact of extended near field is more important for small fire sizes.

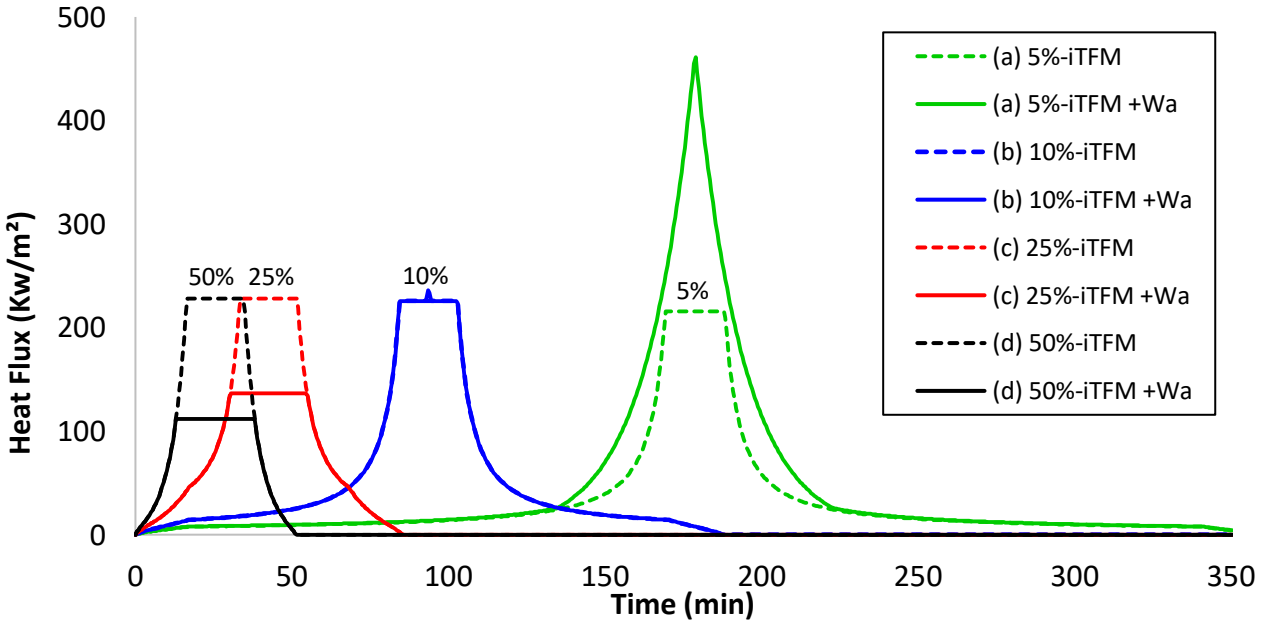

Figure 10 Heat flux received at the level of the ceiling in the middle of the compartment for a family of traveling fire sizes using iTFM and iTFM+Wakamatsu. The impact of extended near field is more obvious for small fire sizes.

Please cite this article as:
Heidari M, Kotsovinos P , Rein G. Flame extension and the near field under the ceiling for travelling fires inside large compartments. Fire and Materials. SPECIAL ISSUE. 2019 :1–14. https://doi.org/10.1002/fam.2773

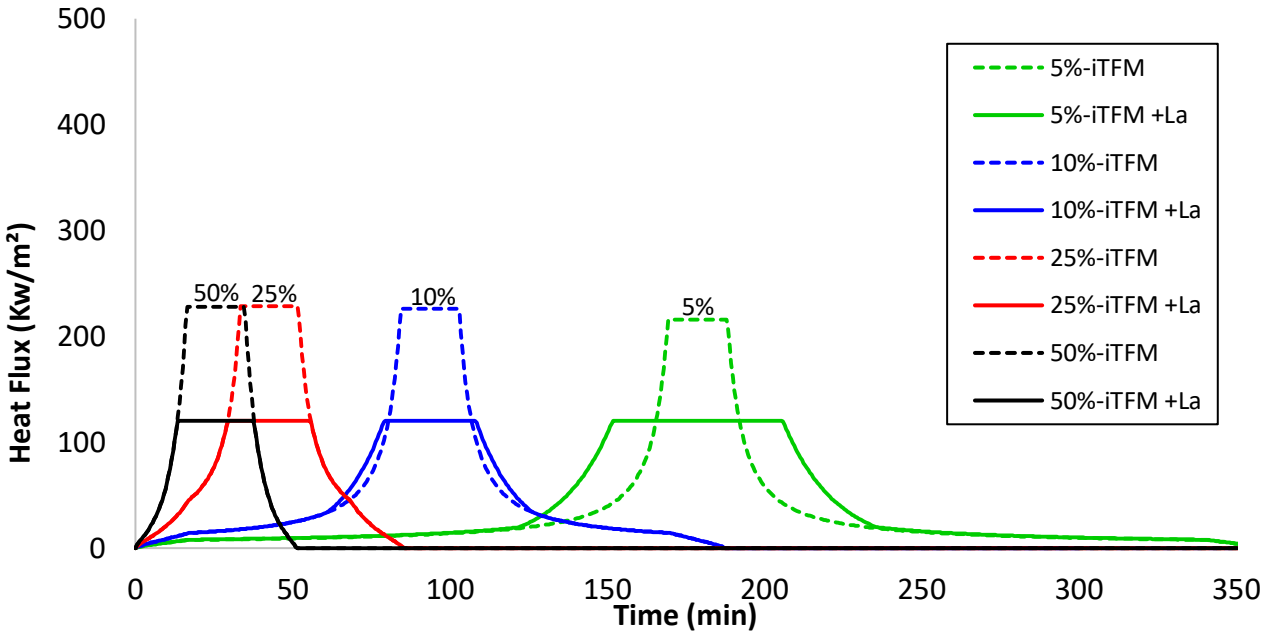

Figure 11 Heat flux received at the level of the ceiling in the middle of the compartment for a family of traveling fire sizes using iTFM and iTFM+Lattimer. The peak heat flux in iTFM+ Lattimer is set to 120 kW/m², in accordance with Lattimer model. The impact of extended near field is more obvious for small fire sizes.

Figure 12 shows the variation of peak heat flux obtained from TFM, TFM+Ha, TFM+Wa and TFM+La for fire sizes of 5% to 50% floor area. The peak heat fluxes decrease or remain constant when the fire size increases, except for TFM without flame extension. This is due to the shorter flame extension under the ceiling and the larger normalized distance of the studied point from the virtual fire source y_t, for the larger fire sizes. On the contrary, the smaller the fire size, the lower peak heat flux calculated from TFM, as shown in Figure 12. This due to the impact of flapping angle in small fire sizes of TFM.

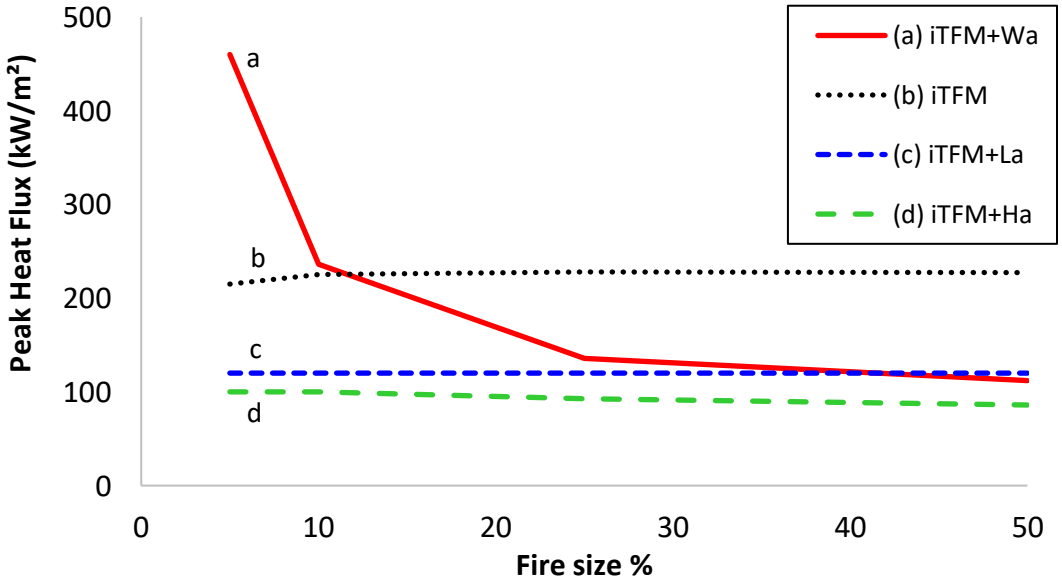

Figure 12 Peak heat flux versus the fire size for TFM with and without flame extension.

Please cite this article as:
Heidari M, Kotsovinos P , Rein G. Flame extension and the near field under the ceiling for travelling fires inside large compartments. Fire and Materials. SPECIAL ISSUE. 2019 :1–14. https://doi.org/10.1002/fam.2773

4.2 Thermal Analysis

Structural fire performance can be evaluated using different performance/failure criteria such as maximum temperature, maximum deflection, the ultimate strain, shear capacity, composite action and continuity within the structure[19,20] depending on the method and objectives of the analysis. Thermal criteria may not always be adequate to conservatively estimate structural fire performance for complex structures. [27,28]

The peak rebar temperature is used as a simple performance criterion to revisit the near field assumption of TFM. The simplified calculation method using the rebar temperature is following the principles described Eurocode 2-1-2[23], as the simply supported slab was subjected to a uniformly distributed load and the design at ambient temperature has been based on linear analysis. This allows determining how travelling fire with flame extension and a heat flux boundary condition could affect the temperature distribution in the structural element. This is illustrated through a comparative study, where TFM and the EN 1991-1-2 parametric fires are also applied. The results of the thermal analysis can be used to identify the worst-case fire scenario and the critical structural members inside the compartment.

The temperature distribution within the steel beams and concrete slab in the middle of the compartment are determined. A family of travelling fires (TFM) ranging from 2.5% to 55%, showed that the 10% fire size results in the highest temperature in the structure at locations further than half of the compartment length from the fire origin.[3] Besides, the impact of flame extension and variation of heat flux were more evident for the 5% fire size, as discussed in the previous section. Therefore, for the purpose of this study, both 5% and 10 % of floor area fire size are examined. Future studies could investigate the impact of all family of travelling fire with flame extension and heat flux boundary condition at all locations in the compartment, using FEM and considering other performance criteria.

Figure 13 and Figure 14 show the resulting temperatures of the steel and concrete members at all times during a fire. Figure 13 shows the temperature for (a) concrete rebar, (b) unprotected and (c) protected steel for a 5% fire size. Figure 14 shows the same for a 10% fire size.

Figure 13 and Figure 14 show that the protected steel beam temperatures and concrete rebar temperatures follow a similar trend. As expected, the unprotected steel beam temperature quickly reaches the near field temperature due to the high conductivity and the low thermal inertia of steel. The maximum temperature obtained for steel and concrete beams are for the 5% fire size. iTFM+Wa results in higher slab and beam temperatures than TFM, for the 5% fire size, and an equal temperature to TFM for the 10% fire size. This is due to the longer near field duration and the greater peak heat flux predicted by iTFM+Wa in comparison with TFM. It should be however noted that as discussed in the previous section, the Wakamatsu model does not have any peak heat flux like the Lattimer and Hasemi models and therefore the results may be unrealistic and overly conservative. This comparative study illustrates that the effect of TFM with flame extension is more important for smaller fire sizes.

Please cite this article as:
Heidari M, Kotsovinos P , Rein G. Flame extension and the near field under the ceiling for travelling fires inside large compartments. Fire and Materials. SPECIAL ISSUE. 2019 :1–14. https://doi.org/10.1002/fam.2773

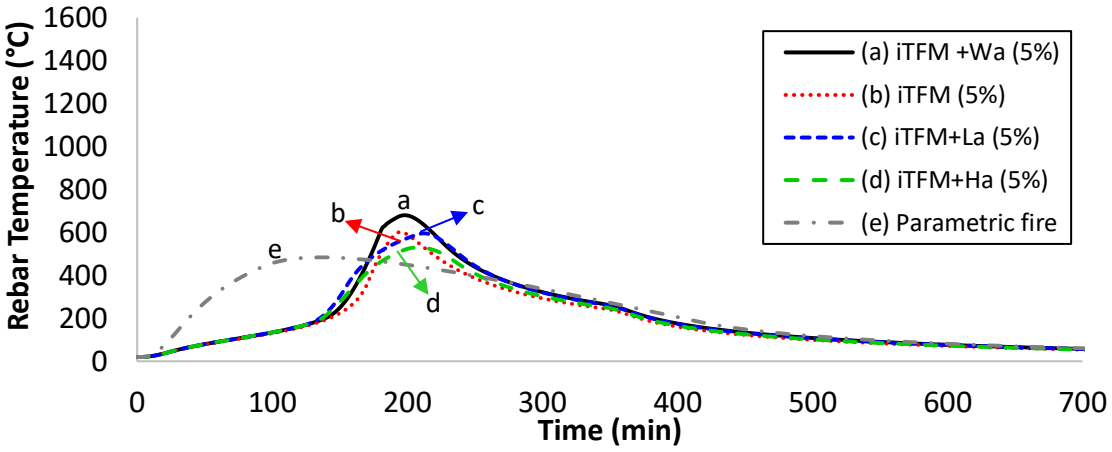

(a)

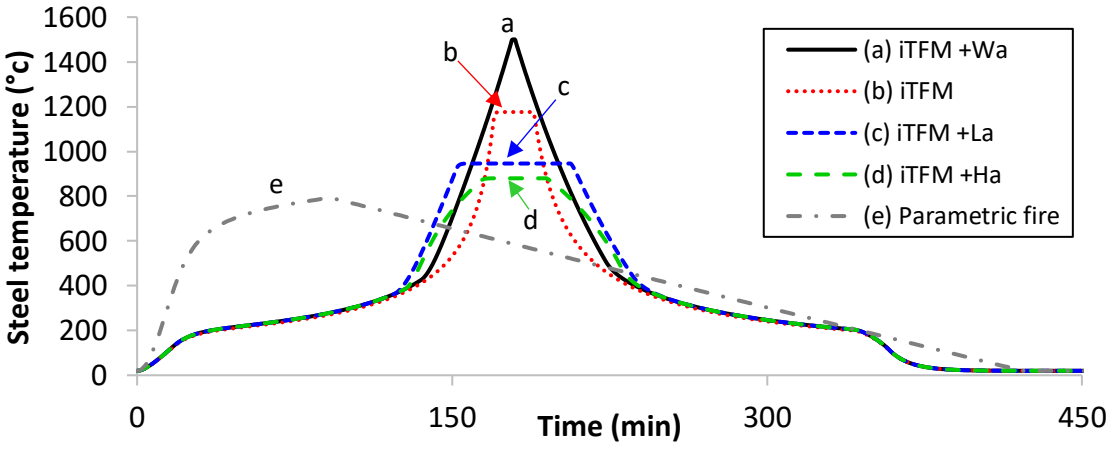

(b)

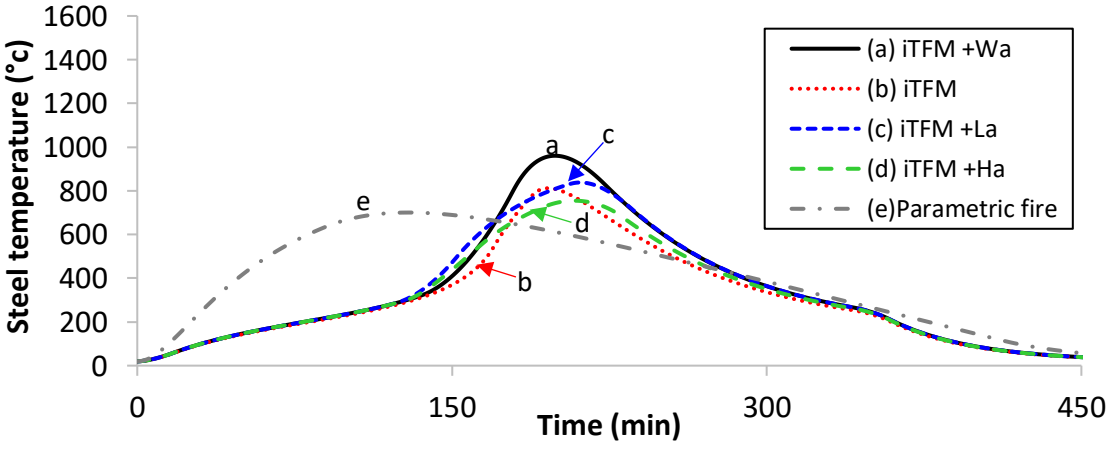

(c)

Figure 13 Comparison of beam temperature curves using parametric fire with 25% ventilation, 5% floor area iTFM without and with and flame extension, for (a) concrete rebar, (b) unprotected and (c) protected steel (R60) beams in the middle of the compartment.

Please cite this article as:
Heidari M, Kotsovinos P , Rein G. Flame extension and the near field under the ceiling for travelling fires inside large compartments. Fire and Materials. SPECIAL ISSUE. 2019 :1–14. https://doi.org/10.1002/fam.2773

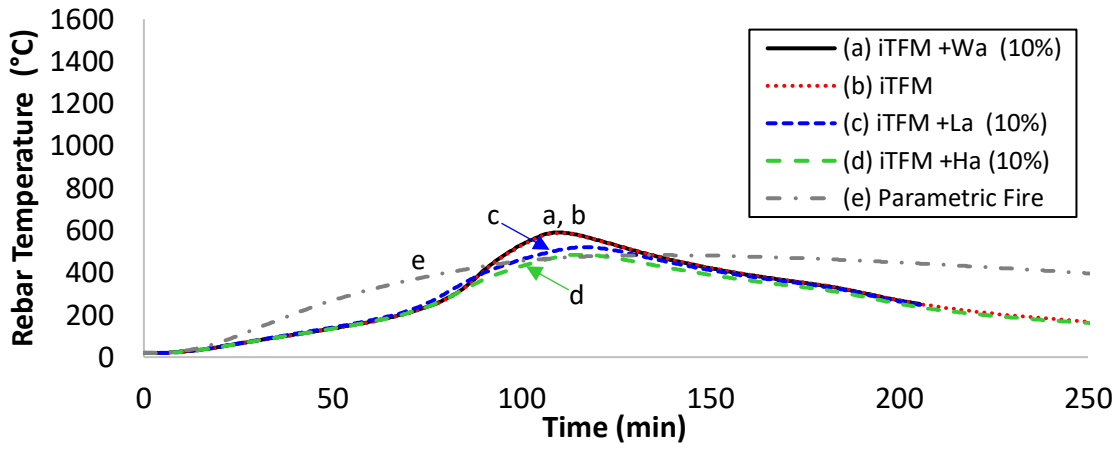

(a)

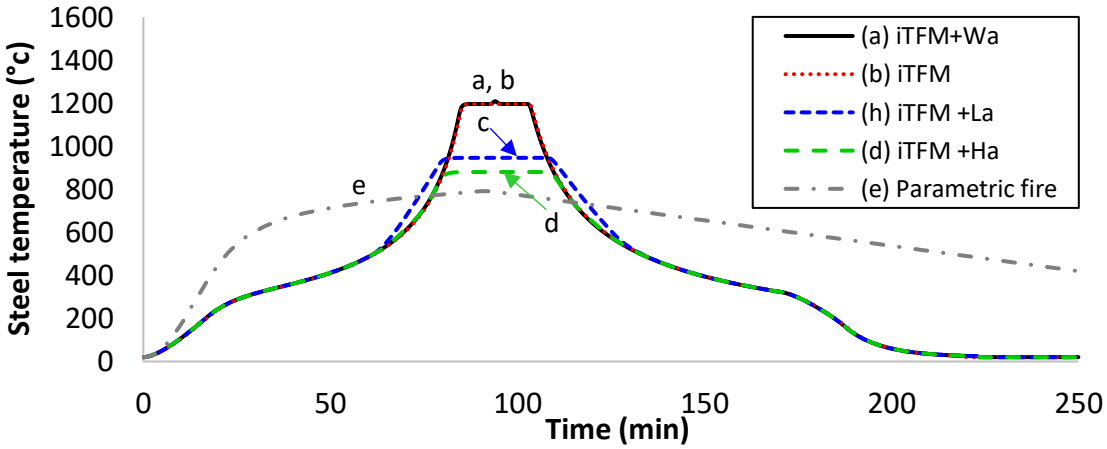

(b)

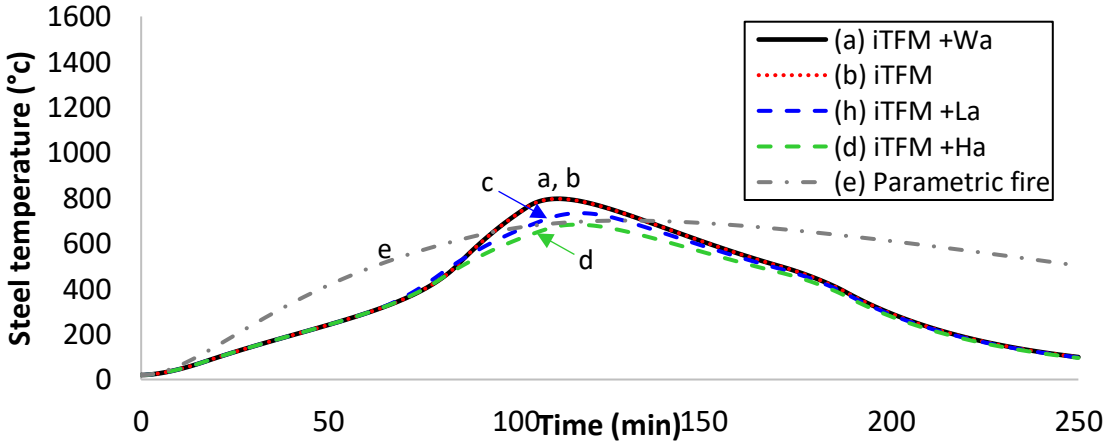

(c)

Figure 14 Comparison of temperature curves using iTFM with and without flame extension with different models, for (a) concrete rebar, (b) unprotected and (c) protected steel (R60) beams in the middle of the compartment, for a fire size of 10% floor area.

Please cite this article as:
Heidari M, Kotsovinos P , Rein G. Flame extension and the near field under the ceiling for travelling fires inside large compartments. Fire and Materials. SPECIAL ISSUE. 2019 :1–14. https://doi.org/10.1002/fam.2773

In the case of the 5% fire size, the iTFM+La has a peak heat flux of 120 KW/m² in comparison with TFM with 215 kW/m² (see Figure 11). However, the resulting peak temperatures of protected steel beam and concrete slab temperatures are similar despite the large differences in heat flux for thermal analysis.

The structural element temperatures using iTFM, fTFM, and EN 1991-1-2 parametric temperature-time curves are compared in Figure 13 and Figure 14. The comparison shows that both TFM with and without flame extension result in peak temperature of structural elements up to 420°C higher than the parametric fire (for 10% fire size).

The results presented in this paper can be explored through a more detailed structural analysis (for example, whole frame behavior) considering different performance criteria, as a travelling fire with flame extension may lead to different structural behavior than that indicated by examining TFM[3] for same fire size or that suggested by the peak temperature of single elements results given here. Further study includes the impact of the family of fire sizes across the compartment.

The peak heat flux from Lattimer correlation is 120 kW/m² and from Hasemi correlation adopted in EN 1991-1-2 is 100 KW/m², which limits the maximum near field prediction of TFM+Ha and TFM+La. Further sensitivity analysis needed on the peak heat flux at the ceiling level. It should be noted that the presented methodology could be updated when more experimental data are available. The study shows that the TFM near field model can be used conservatively to assess thermal response for structural design purposes provided that a suitable range of fire sizes is selected. Future experiments in large compartments are needed to further improve the near field model.

5 CONCLUSION

The travelling fire methodology (TFM) characterizes the thermal boundary condition where fire travels across the compartment floor plate leading to fire durations of several hours and a non-uniform thermal environment inside the compartment. TFM is a design tool based on simplified assumptions and therefore this paper revisits its near field assumptions.

This work for the first time considers the flame extension under the ceiling for the near field region of travelling fires, which affects the heating exposure to the structural members. This paper also for the first time formulates the TFM in terms of heat flux rather than temperatures, thus allowing for a more formal heat transfer boundary condition between the gas and the surface of the structural element. The Hasemi, Wakamatsu and Lattimer models are used to determine the heat flux received at the level of the ceiling. The presented methodology is applied to an office compartment of 960 m² floor area and 3.60 m high with concrete and protected and unprotected steel structural members. The analyses compare the thermal response of the concrete slab and steel structural beams when subjected to iTFM, the travelling fire models with flame extension and the EN 1991-1-2 parametric fire curve, which assumes uniform temperature and a uniform burning condition.

Please cite this article as:
Heidari M, Kotsovinos P , Rein G. Flame extension and the near field under the ceiling for travelling fires inside large compartments. Fire and Materials. SPECIAL ISSUE. 2019 :1–14. https://doi.org/10.1002/fam.2773

Travelling fires with flame extension, lead to an increase in the length of the near field. For a 5% fire size, the near field with flame extension is 12.8 m where the near field length from iTFM is 2m. The near field length with and without flame extension for a 25% fire size is 26.8 m and 10 m respectively. The analysis illustrated that the smaller the fire size, the larger impact of flame extension on the near field length.

The study established that formulating the near field in terms of heat flux is correct and accurate. The peak heat flux of small fires sizes, using flame extension and the Wakamatsu model is larger the one calculated with TFM. Flame extension with the Lattimer model and the Hasemi model result in a lower peak heat flux than TFM. The time that the structural element is heated by the peak heat flux varies between different models and fire sizes. For a 5% floor area fire TFM+ Lattimer has the largest duration of 52 min, TFM+Hasemi and TFM had 28 min and 17 min respectively. The study shows that the near field duration depends on the length of flame under the ceiling, rather than the local burning time of TFM. The smaller the fire size, the longer the near field duration. This could affect the resulting temperature of the structural elements and structural behavior. Although outside the scope of this paper, formulating the thermal boundary condition in terms of heat flux would allow determining the thermal behavior of any structural material, including timber structures.

The study shows that for all cases, TFM results in higher structural temperatures except for the Wakamatsu model, which leads to approximately 20% higher temperatures than TFM. However, the analysis has shown that the time to structural failure can be earlier when the flame extension is considered for small fire sizes.

The comparison for the generic arrangement studied in this work, with the EN 1991-1-2 parametric curve illustrates that the peak temperatures resulting from parametric fire are 484°C at the concrete rebar, 700°C for protected steel beam and 791°C for unprotected steel beam. For a 10% floor area travelling fire with flame extension and different models, the resulted peak temperature varies between 485°C and 590°C at the concrete rebar, 680°C and 800°C in the protected steel beam, and 880°C and 1200°C in the unprotected steel beam. Regardless of the near field model, TFM results in higher temperatures in the structure than parametric fire. Therefore, it is concluded that the EN 1991-1-2 parametric fire is less conservative, and the design of the structural elements is controlled by the TFM scenario.

These findings mitigate the uncertainty around the shortcomings of the TFM near field model and reinforce that it can be conservatively used for the assessment of the thermal response of structures. The development of the presented methodology (fTFM) is analogous to that of the previous versions of the travelling fire methodology,[2,3,5] that is already used as a complementary tool in design practice,[6,7] and therefore fTFM could also be used for design purposes.

Acknowledgements

The authors appreciate the support of CERIB, Arup and Imperial College who helped to develop this work.

References:

1. Stern-Gottfried J, Rein G. Travelling fires for structural design – Part I : Literature review. *Fire Saf J*. 2012;54:74-85. doi:10.1016/j.firesaf.2012.06.003

2. Stern-Gottfried J, Rein G. Travelling fires for structural design-Part II: Design methodology. *Fire Saf J*. 2012;54:96-112. doi:10.1016/j.firesaf.2012.06.011 mj_heidari@yahoo.com.

3. Rackauskaite E, Hamel C, Law A, Rein G. Improved Formulation of Travelling Fires and Application to Concrete and Steel Structures. *Structures*. 2015;3:250-260. doi:10.1016/j.istruc.2015.06.001

4. Rackauskaite E, Kotsovinos P, Jeffers A, Rein G. Structural analysis of multi-storey steel frames exposed to travelling fires and traditional design fires. *Eng Struct*. 2017. doi:10.1016/j.engstruct.2017.06.055

5. Law A, Jamie Stern-Gottfried J, Gillie M, Rein G. THE INFLUENCE OF TRAVELLING FIRES ON THE RESPONSE OF A CONCRETE FRAME. In: *International Conference of Structure.Lansing,Michigan,USA*. Lansing,Michigan,USA; 2010.

6. Block F., Kho T. Engineering an icon or the probabilistic-based structural fire engineering of the Battersea power station. In: *9M.E.M. Garlock, V.K.R. Kodur (Eds.), Proc. 9th Int. Conf. Struct. Fire, Princeton, NJ, DEStech Publications*. ; 2016:901-908.

7. Law A, Stern-Gottfried J, Butterworth N. A Risk Based Framework for Time Equivalence and Fire Resistance. *Fire Technol*. May 2014. doi:10.1007/s10694-014-0410-9

8. Alpert R. Model-Based Analysis of a Concrete Building Subjected to Fire. *Fire Technol*. 1972;Vol 83(Issue: 3):181-195.

9. Alpert RL. Ceiling Jet Flows. In: *SFPE Handbook of Fire Protection Engineering, Fifth Edition*. New York, NY: Springer New York; 2016:429-454. doi:10.1007/978-1-4939-2565-0_14

10. Rackauskaite E, Fernandez-Anez N, Bonner M, et al. x-ONE Fire Experiment in a Very Large and Open-Plan Compartment. In: *SFPE 12th International Conference on Performance Based Codes and Fire Safety Design Methods*. Honolulu, Oahu; 2018.

11. Hidalgo JP, Goode T, Gupta V, et al. The Malveira fire test: Full-scale demonstration of fire modes in open-plan compartments. *Fire Saf J*. 2019;108:102827. doi:10.1016/J.FIRESAF.2019.102827

12. ISO 834-1:1999(en), Fire-resistance tests — Elements of building construction — Part 1: General requirements. https://www.iso.org/obp/ui/#iso:std:iso:834:-1:ed-1:v1:en. Accessed February 6, 2019.

13. Eurocode 1. *Actions on Structures —Part 1-2: General Actions — Actions on Structures Exposed to Fire*. Vol 3. European standard EN 1991-1-2, CEN, Brusseles; 2002.

14. Drysdale D. *An Introduction to Fire Dynamics*. Chichester, UK: John Wiley & Sons, Ltd; 2011. doi:10.1002/9781119975465

15. Torero JL, Law A, Maluk C. Defining the thermal boundary condition for protective structures in fire. *Eng Struct*. 2017;149:104-112. doi:10.1016/J.ENGSTRUCT.2016.11.015

16. Babrauskas V. Flame lengths under ceilings. *Fire Mater*. 1980;4(3):119-126. doi:10.1002/fam.810040304

17. Hasemi Y, Yokobayashi S, Wakamatsu T, Ptchelintsev A. Fire safety of building components

exposed to a localized fire- scop and experiments on ceiling/beam system exposed to a localized fire. In: *ASIAFLAM '95 : 1st International Conference.* InterScience Communications; 1995. https://openlibrary.org/books/OL17168996M/ASIAFLAM_'95. Accessed February 6, 2019.

18. Lattimer BY. SFPE Handbook of Fire Protection Engineering,Fifth Edition, Heat Transfer from Fires to Surface. In: *SFPE Handbook of Fire Protection Engineering (5th Edition),*. ; :745. doi:10.1007/978-1-4939-2565-

19. Franssen J-M, Cajot L. Natural Fires in large compartment, Effects caused on the structure by localised fires in large compartments. 1998.

20. J. Myllymaki and M. Kokkala. *"Thermal Exposure to a High Welded I-Beam Above a Pool Fire," First International Workshop on Structures in Fires*. Copenhagen; 2000. http://www.structuresinfire.com/corpo/conferences/sif00.pdf.

21. Incropera FP, DeWitt DP, Bergman TL, Lavine AS. *Fundamentals of Heat and Mass Transfer*. Vol 6th. (Incropera FP, Incropera FPFOHAMT, eds.). John Wiley & Sons; 2007. http://www.osti.gov/energycitations/product.biblio.jsp?osti_id=6008324.

22. Buchanan AH. *Structural Design for Fire Safety*. Chichester, UK,Wiley & sons; 2002.

23. Eurocode 2. *Design of Concrete Structures-Part 1-2: General Rules — Structural Fire*. European Standard EN 1992-1-2,CEN,Brussels; 2004.

24. Eurocode 3. *Design of Steel Structures - Part 1-2: General Rules - Structural Fire Design*. Vol 2. European Standard EN 1993-1-2,CEN,Brussels; 2011.

25. Heidari M, Robert F, Lange D, Rein G. Probabilistic Study of the Resistance of a Simply-Supported Reinforced Concrete Slab According to Eurocode Parametric Fire. *Fire Technol*. March 2018:1-28. doi:10.1007/s10694-018-0704-4

26. Stern-gottfried J. Travelling Fires for Structural Design.Ph.D thesis. 2011. doi:10.1016/j.firesaf.2012.06.003

27. Rackauskaite E, Kotsovinos P, Jeffers A, Rein G. Computational analysis of thermal and structural failure criteria of a multi- storey steel frame exposed to fire. *Eng Struct*. 2019;180(November 2018):524-543. doi:10.1016/j.engstruct.2018.11.026

28. *ISO/DTR 24679-6 Fire Safety Engineering -- Performance of Structures in Fire - Part 6: Example of an Eight-Storey Reinforced Concrete Building*. Geneva,Switzeralnd (In press); 2015.